



Analysis of quantization error in high-precision continuous-flow isotope ratio mass spectrometry

Gavin L. Sacks, Christopher J. Wolyniak, J. Thomas Brenna*

Savage Hall, Division of Nutritional Sciences, Cornell University, Ithaca, NY 14853, USA

Received 10 June 2003; received in revised form 8 August 2003; accepted 12 August 2003

Abstract

High-precision isotope ratio mass spectrometry (IRMS) systems are equipped with digitizers that deliver effective maximum digitization depths of 16 to 24 bits; however, there are no analyses of the proper board depth required to retain high precision in continuous-flow techniques. We report an experimental and theoretical evaluation of quantization error in continuous-flow IRMS (CF-IRMS). CO₂ samples (100 pmol–30 nmol) were injected into a gas chromatography combustion IRMS system (GC-CIRMS). The analog signal was digitized by high precision, 24-bit ADC boards at 10 Hz, and was post-processed to simulate 12, 14, and 16-bit data sets. $\delta^{13}\text{C}_{\text{pdb}}$ values were calculated for all data sets by the conventional “summation” method or by curve-fitting the chromatographic peaks to the exponentially modified Gaussian (EMG) function. Benchmarks of S.D. ($\delta^{13}\text{C}_{\text{pdb}}$) = 0.3, 0.6, and 1.0‰ were considered to assess precision. In the presence of significant quantization noise, curve-fitting required several-fold less CO₂ than the summation method to reach a given benchmark. We derived an equation to describe the theoretical limitations of precision for the summation method as a function of CO₂ admitted to the source and the step size of the boards. Theory was in close agreement with the observed lower limit of precision for the simulated 16-bit data set. Curve-fitting achieved a precision of S.D. <0.3‰ for injections 20-fold smaller than summation for CO₂ samples collected on an IRMS with 16-bit resolution. By mitigating the impact of quantization noise, curve-fitting expands the dynamic range within a single run to include lower analyte levels, and effectively reduces the need for high pumping capacities and high precision ADC boards.

© 2003 Elsevier B.V. All rights reserved.

Keywords: Isotope ratio mass spectrometry; Mass spectrometry; Quantization error; Carbon dioxide

1. Introduction

Isotope ratio mass spectrometry (IRMS) coupled to a gas chromatography–combustion interface (GC–C) can routinely measure relative differences in ¹³C/¹²C isotope ratios to a precision of few parts per million for samples containing 10 ng of sample or less

[1,2]. GC–CIRMS data consists of three concurrent chromatographic traces (⁴⁴CO₂, ⁴⁵CO₂, ⁴⁶CO₂) from three detectors operated in parallel. Achieving high precision requires careful and consistent definition of background levels and peak integration for all three traces. Most commonly, peak areas are integrated by the “summation” method. The start and end of a peak are detected, and the background is described as a square or trapezoidal area beneath the peak. Raw data are summed over the length of the peak, and the background area is subtracted. Ricci et al. [3] described two

* Corresponding author. Tel.: +1-607-255-9128;
fax: +1-607-255-1033.

E-mail address: jtb4@cornell.edu (J.T. Brenna).

general methods for determining the background using summation; the “individual summation” method, in which the background is defined by connecting low points on either side of the peak, and the “dynamic summation” method, in which low points are connected throughout the chromatogram regardless of the location of peaks.

All IRMS instruments use digitizers to convert analog signal from Faraday cups to digital data, which must be processed to yield isotope ratios. The precision of a digitizer is expressed in terms of bits, where an N -bit board has 2^N steps over a given range. As an example, a 16-bit board has $\sim 65\,000$ steps; if the board has a range of 0–10 V, then the step size of the board is ~ 0.15 mV. The rounding of a continuous signal to discrete steps introduces noise, which is referred to as quantization error or “bit noise”. This effect is shown graphically in Fig. 1, where simulated Gaussian peaks of 24, 16, 14, and 12-bit resolution are presented. At high resolution (24 bits), no quantization noise is noticeable, and the peak appears as a smooth trace. As the resolution decreases, steps become obvious, and the shape of the peak deteriorates. The quality of data reduction in continuous-flow IRMS must depend at least in part on the digitizer depth because the intensity level established for peak start and stop depends on this parameter. As depth decreases, the intensity of

the background is, in general, less well represented by the intensity levels of the peak’s start and stop points. There are no analyses available that establish the relationship between isotope ratio precision and digitization depth.

The effect of digitization depth on precision and accuracy is inextricably linked to data reduction algorithms. The reproducibility of the summation background correction depends in part on the two points that anchor the background line under the peak; imprecision in the measurement of either point multiplies through the entire length of the background segment connecting the points. In the presence of a simple linear background, a background line is easily drawn between any two points on either side of the peak, as shown in Fig. 2a. Chemical noise due to column bleed or contaminant peaks may cause inaccuracy in defining the background, but such noise is usually correlated in all three traces. This covariance may mitigate the effects of chemical noise on the calculated isotope ratio. However, in the case of quantization error, as shown in Fig. 2b, the magnitude and direction of error is uncorrelated among the three traces, and this then poses a special case. Our previous work has shown that peak integration by curve-fitting improves precision and accuracy in cases of low signal-to-noise [4] and overlapping peaks [5]. Background correction

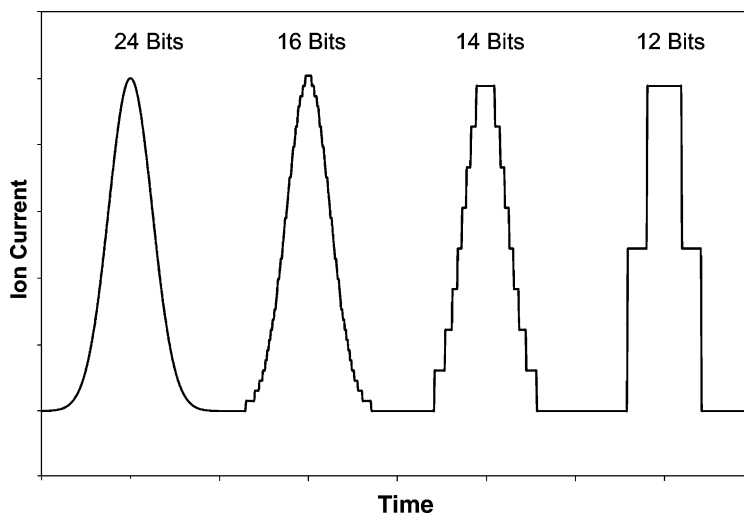


Fig. 1. A simulation of a Gaussian signal collected by ADCs of various resolutions (24, 16, 14, and 12 bits) and quantization errors. At 24-bit resolution, quantization error is not visible, and the peak appears as a smooth trace. At 16 bits, bit noise is evident primarily at the base of the peak. At 12-bit resolution, the signal is barely recognizable as a Gaussian shape.

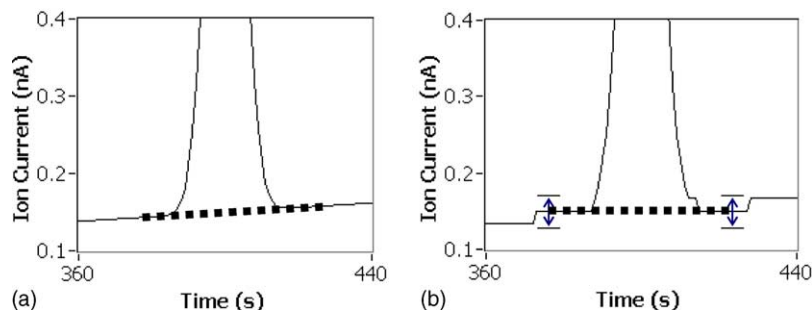


Fig. 2. Simulated chromatographic peaks in the presence of a linearly rising background (a) without and (b) with quantization error. In the presence of quantization error, the true background may fall anywhere within the arrows. Without quantization error background is easily and accurately achieved by connecting points on either side of the peak.

in curve-fitting is not constrained to the actual values represented by the discrete digitization levels, and we hypothesized that it may not be as sensitive to quantization error as summation.

Quantization error is typically not dominant in GC–CIRMS when high precision IRMS data acquisition systems use sufficiently deep digitization boards and signals are sufficiently strong. Noise from other sources, such as chemical noise, is greater than the step size of the digitizers. However, quantization error may become important in two specific situations: (a) in data reduction of minor peaks in a chromatogram where there are fewer steps between baseline and peak top, and (b) when low precision digitizers are used, as is common in low cost IRMS instruments designed primarily for measurements of high abundance samples, such as CO_2 in breath tests. In addition, these systems usually have lower pumping capacity, which limits the flow rate that the IRMS source accepts. The lower inlet flow rates result in smaller signals for equivalent analyte abundance via higher split ratios, making quantization error more prominent. In this report, we evaluate quantization error theoretically and experimentally to determine the limiting the precision achieved by the conventional summation algorithm and by curve-fitting.

2. Experimental

2.1. Instrumentation

A Varian 3400 GC system was coupled via a combustion furnace to one of two gas IRMS instruments:

(a) a FinniganMAT 252 (FMAT252) run in high linearity mode, or (b) an Analytical Precision Products 2003 (APP2003). Both IRMS systems were operated with a source pressure of 1×10^{-6} Torr and had an absolute sensitivity of ~ 5000 mol/ion (1 Torr = 133.322 Pa). The GC–C system is described in detail elsewhere [6]. Briefly, the effluent from the capillary column (60 m \times 0.32 mm, 0.25 μm , BPX70; SGE, Austin, TX, USA) is directed to a combustion furnace filled with CuO and held at 850 $^\circ\text{C}$, and dried in a Nafion water trap before admittance to the IRMS system through an open split. Since CO_2 gas was injected as a sample, the combustion step was not necessary, but was retained in the system to increase the verisimilitude to real GC–CIRMS operating conditions. The FMAT252 has differential pumping and a higher overall pumping capacity, while the APP2003 has only a single turbopump. As a result, the FMAT252 can tolerate higher inlet flow rates. The open split of the FMAT 252 accepted 0.2 ml/min (split ratio = 8.4:1), and the open split of the APP2003 accepted 0.07 ml/min (split ratio = 24:1).

CO_2 (Airgas East, 99.9%) injections were performed by hand consecutively. The split ratio and the injection size were varied to yield between 100 pmol and 30 nmol on column. Four or five replicates were performed for each injection size. The moles of CO_2 in each injection were approximated by assuming ideal gas conditions.

Data was collected on the FMAT 252 using SAXI-CAB [7], a laboratory-built LabVIEW-based [8] data acquisition system employing National Instruments (Austin, TX, USA) 435 \times digitizers yielding

24 bits operating at 10 Hz. Data were collected on the APP2003 using the vendor-supplied 16-bit, 10 Hz data acquisition system. Both systems simultaneously monitored the $m/z = 44, 45,$ and 46 cups with $>99\%$ duty cycle.

2.2. Data processing

Before data reduction, data collected from the FMAT 252 at 24 bits was rounded on all three traces to simulate 16-, 14-, and 12-bit data sets. The head amplifiers have a maximum signal of 10 V (33 nA for $m/z = 44$), so the step size, Δ , for a given board depth was calculated as:

$$\Delta = \frac{10 \text{ V}}{2^{\text{bits}}} \quad (1)$$

We created simulated data sets by rounding data points to the nearest step:

$$\text{data(quantized)} = \text{round} \left[\frac{\text{data(raw)}}{\Delta} \right] \Delta \quad (2)$$

where, the *round* function rounds the input to the nearest whole number.

The 16-bit data from the APP2003 was used without modification. All data sets were processed using SAXICAB by either the individual summation method or by curve-fitting. The individual summation method used by SAXICAB was adapted from Ricci et al. [3]. Starts and stops of peaks were determined with a slope sensitivity of 0.3 nA/s. The lowest point 2 s before and 2 s after the peak limits were located, and a straight line was drawn between the two points to define the background. In the curve-fitting algorithm, the traces were fit to exponentially modified Gaussian (EMG) functions using the Levenberg–Marquardt algorithm. Mathematical details of the EMG function can be found elsewhere [9].

High-precision isotope ratios are expressed in the delta (‰) notation:

$$\delta^{13}\text{C}_{\text{pdb}} = \frac{{}^{13}R_{\text{spl}} - {}^{13}R_{\text{pdb}}}{{}^{13}R_{\text{pdb}}} \times 1000 \quad (3)$$

where ${}^{13}R_x$ is the ratio of ${}^{13}\text{C}$ to ${}^{12}\text{C}$, SPL refers to the sample, and PDB refers to the international standard, PeeDee Belemnite, where ${}^{13}R_{\text{pdb}} = 0.0112372$. In our work, $\delta^{13}\text{C}$ of the CO_2 injections were calculated using pulses of standard CO_2 gas that had been indirectly

calibrated to the PDB reference. The contribution of ${}^{17}\text{O}$ to the ${}^{45}\text{CO}_2$ signal was taken into account by the method of Santrock et al. [10]. No outliers were excluded from the reported data.

3. Results and discussion

3.1. Observed effects of quantization error

Fifteen CO_2 injection amounts were used to produce peak areas on the FMAT 252 that varied over 2.5 orders of magnitude. The peaks showed excellent symmetry and narrow peak widths, with a full width at half maximum of <3 s. The mean reproducibility of the area for each injection size, as measured by the area of the $m/z = 44$ signal, was R.S.D. = 13%. Plots of $\delta^{13}\text{C}_{\text{pdb}}$ versus injection size, shown in Fig. 3, are displayed for both the curve-fitting (a) and individual summation (b) methods. The plots are similar in appearance to those presented by others [11] investigating the performance of GC–CIRMS at low signal levels.

In agreement with our previous work [4], we observe modest improvement of precision at low signal levels using the curve-fitting method. Using the summation method, precision deteriorates (S.D. $> 1.0\%$) for injection sizes less than 400 pmol on column (~ 50 pmol to the IRMS). Curve-fitting improves this limit to 175 pmol on column (~ 20 pmol to the IRMS). The integration methods performed comparably and acceptably at large injection sizes. For on-column injections of at least 6.8 nmol (~ 800 pmol to the IRMS), the individual summation method had a precision of S.D. ($\delta^{13}\text{C}_{\text{pdb}}$) = 0.1‰. The curve-fitting method gave slightly worse precision for large injections, S.D. ($\delta^{13}\text{C}_{\text{pdb}}$) = 0.2‰. It is not obvious why the summation method out-performs the curve-fitting method for very large sample sizes. One possibility is that the precision of the curve-fitting method is limited by differences between the shape of the model EMG function and the shape of real, chromatographic peaks. In this case, increasing the injection size past a certain point would not improve the fit, even though S/N is increasing. Using a different function to describe the peaks may further improve results.

To assess the tolerance of the two integration methods to quantization noise, we evaluated simulated

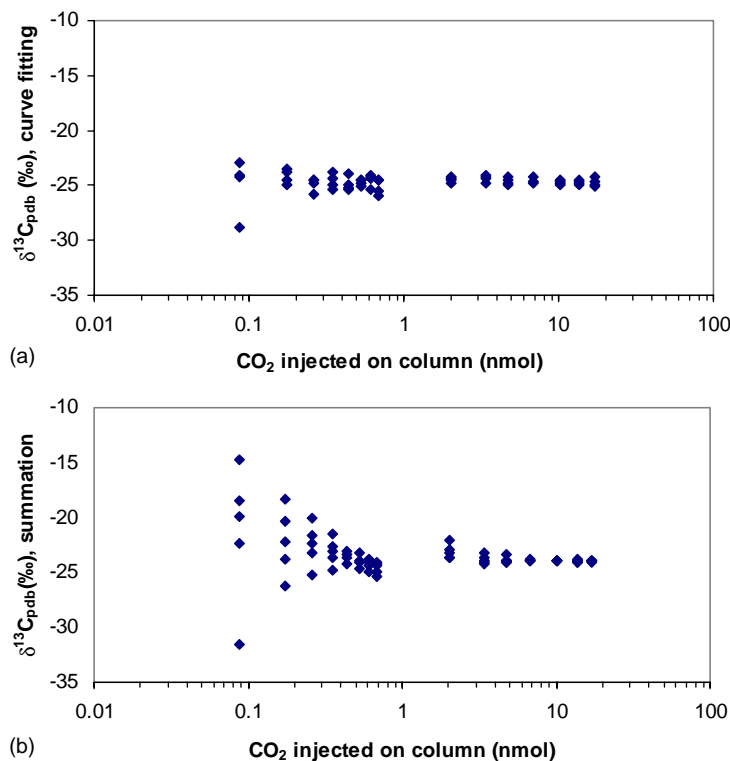


Fig. 3. $\delta^{13}\text{C}_{\text{pdb}}$ vs. CO_2 injected on column for (a) curve-fitting and (b) individual summation algorithms. Data was collected using a homebuilt system at 24 bits from FMAT252.

12, 14, and 16-bit raw data sets generated from the raw 24-bit FMAT252 data, and processed both by curve-fitting and summation. The accuracy of successive injections was very good, even in the presence of bit noise. For each method, the mean $\delta^{13}\text{C}$ for any two injection sizes did not differ significantly. Plots of $\text{S.D.}(\delta^{13}\text{C}_{\text{pdb}})$ versus CO_2 injected on column at all bit resolutions are shown in Fig. 4. Each plot appears to extend asymptotically along the x - and y -axes, and we can evaluate the dependence of precision on quantization error visually; poor performance is indicated by the asymptotic plot moving up and away from the axes. At 24-bit resolution, plots of the summation and curve-fitting methods nearly overlap, except at very small injection amounts, indicating that performance is similar. With increasing quantization error, the minimum amount of CO_2 necessary to reach a given level of precision increases rapidly for the summation method. Curve-fitting is more forgiving; precision from 14- and 16-bit data is comparable to

the 24-bit data. The plot for 12-bit resolution shows some loss of precision, but does not fare as badly as the summation method.

To evaluate the methods objectively, we defined $\text{S.D.}(\delta^{13}\text{C}_{\text{pdb}}) = 0.3, 0.6$ and 1.0% as benchmarks for high precision. The data were least-squares fitted to a power function, of the form:

$$\text{S.D.} = A[\text{CO}_2]^B \quad (4)$$

where $[\text{CO}_2]$ is the moles of CO_2 injected on column, S.D. is the observed precision, and A and B are constants. The power function was chosen for empirical reasons, because it modeled the observed data acceptably, and the fitted curves can then be compared. The best-fit lines for both the summation (dashed) and curve-fitting (solid) methods are shown in Fig. 4. From the best-fit equations, we calculated the amount of CO_2 injected on-column necessary to achieve the 0.3, 0.6, and 1.0% benchmarks (Fig. 5). With least quantization error (24-bit resolution), the

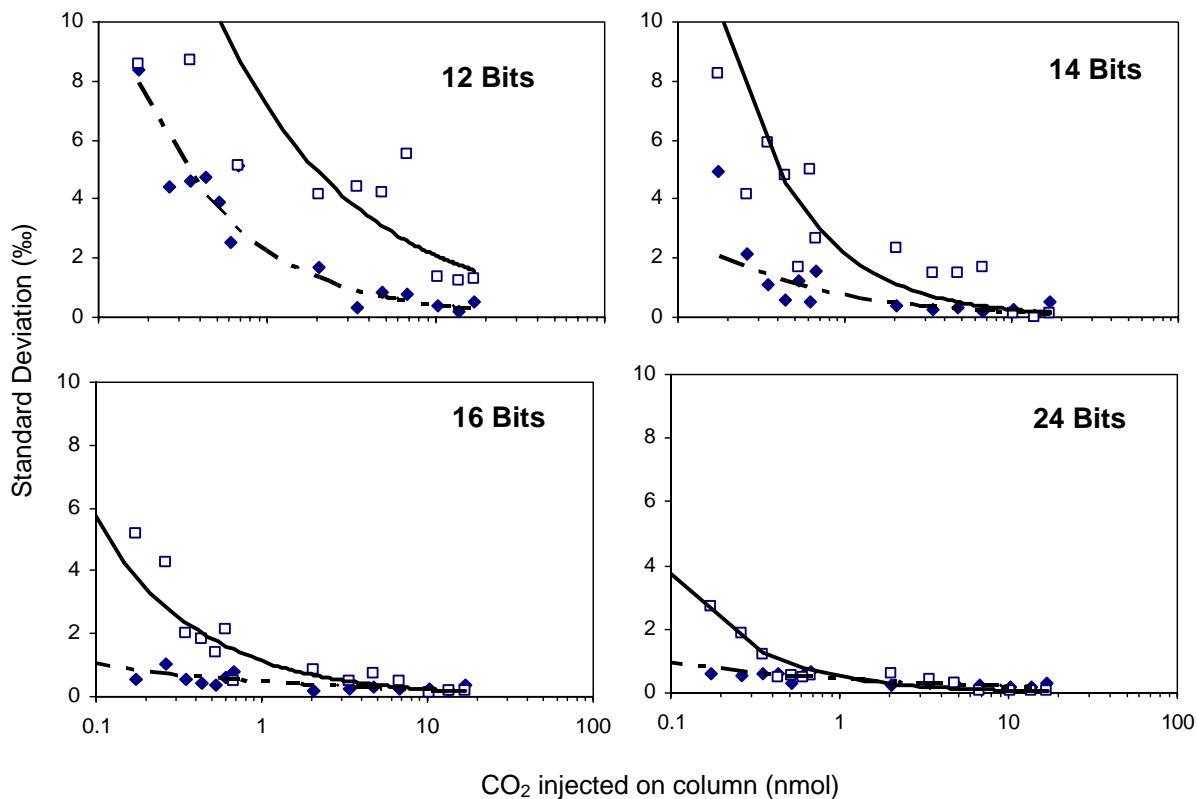


Fig. 4. S.D. ($\delta^{13}\text{C}_{\text{pdb}}$) vs. CO_2 injected on column at 12-, 14-, 16-, and 24-bit resolutions, calculated by summation (\square) or curve-fitting (\blacklozenge) algorithms. Each point represents four or five replicates. The data for each method and each resolution was fit to a power equation (general form: $\text{S.D.} = A[\text{CO}_2]^\beta$, and the best-fit lines are drawn for both methods (solid line: summation; dashed line: curve-fitting).

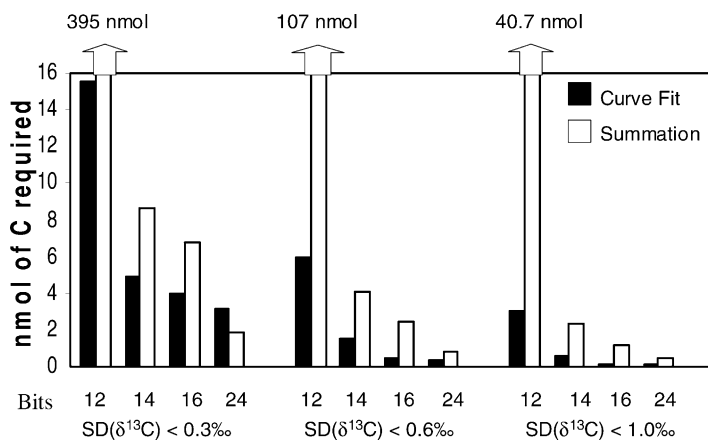


Fig. 5. Carbon required on-column, in nanomoles, to reach a specified level of precision for a given ADC board resolution. Results are shown for data reduced by curve-fitting and summation algorithms.

summation method requires slightly less CO₂ than the curve-fitting method at the 0.3‰ benchmark (1.86 nmol versus 3.19 nmol). At 16-bit resolution, the summation method requires 6.83 nmol, an increase of 267%, compared to a 25% increase for curve-fitting over the same interval. To reach the 0.6‰ benchmark at 16 bits, summation requires an increase of 224% (from 0.77 to 2.50 nmol), compared to 33% for curve-fitting. At 12-bit resolution, the amount of CO₂ on column necessary to achieve S.D. = 0.6‰ by summation is 107 nmol, which far exceeds the capacity of the GC column. Curve-fitting requires only 6 nmol to reach S.D. = 0.6‰ at 12-bit resolution. As was discussed previously, curve-fitting is superior to summation at the 1.0‰ benchmark, even in the absence of quantization noise. At 24 bits, curve-fitting requires 80 pmol to achieve S.D. = 1.0‰, five-fold less than summation; a similar level of improvement in precision is seen at 14- and 16-bit resolution.

To summarize, in the absence of quantization noise, similar amounts of CO₂ are necessary to achieve precision of 0.3–0.6‰ for both integration methods. The summation method requires a dramatic increase in the injection size to maintain this level of precision in the presence of quantization noise, while the curve-fitting method is relatively unaffected. At a lower standard of precision (S.D. = 1.0‰), curve-fitting is superior regardless of the magnitude of quantization error.

3.2. Theoretical limits of quantization error on precision

In IRMS, the signal is recorded as a voltage proportional to the ion current, and can be reported in amperes or in volts. If the signal is reported in volts, the area of the $m/z = 44$ signal, A_{44} , is related to the moles of ⁴⁴CO₂ that enters the IRMS, [⁴⁴CO₂], by the equation:

$$A_{44} = [{}^{44}\text{CO}_2] \frac{N_a e}{E} R_\Omega \quad (5)$$

where N_a is Avogadro's number, e is the fundamental charge, E is the absolute sensitivity of the IRMS in molecules/ion, and R_Ω is the feedback resistance of the amplifier.

In the summation method, the background is defined by drawing a line between two background points, (t_1, y_1) and (t_2, y_2) ; the background area, A , is the

trapezoidal region between this line and the time axis. We can calculate this area by the equation:

$$A(\text{background}) = \frac{1}{2} W(y_1 + y_2), \quad (6)$$

where $W = t_2 - t_1$

Quantization noise is uniformly distributed over an interval and the error for a single measurement is:

$$\sigma_y = \frac{\Delta}{\sqrt{12}} \quad (7)$$

where Δ is the minimum step size of the acquisition boards. A full derivation of this can be found in Haykin's text on digital communication [12]. Assuming that quantization error at y_1 and y_2 is uncorrelated, we can use standard techniques for propagation of errors to determine the total quantization error in measuring the background area, σ_A :

$$\sigma_A = \frac{W\Delta}{2\sqrt{6}} \quad (8)$$

It has been noted that evaluating the effect of chemical noise on precision of isotope ratios is difficult, because this noise is usually highly correlated between the major and minor traces [11]. Unlike chemical noise, quantization noise on each trace should be uncorrelated. This greatly simplifies calculation of the propagation of errors for the relation of the observed isotope ratio, ⁴⁵R_{obs}, to the actual isotope ratio, ⁴⁵R_{act}:

$${}^{45}R_{\text{obs}} = \frac{A_{45} \pm \sigma_{45}}{A_{44} \pm \sigma_{44}} = {}^{45}R_{\text{act}} \pm \sigma_{\text{obs}} \quad (9)$$

where

$$\sigma_{\text{obs}} = {}^{45}R_{\text{act}} \sqrt{\left(\frac{\sigma_{45}}{A_{45}}\right)^2 + \left(\frac{\sigma_{44}}{A_{44}}\right)^2} \quad (10)$$

The standard error can be rearranged and expressed in terms of parts per thousand:

$$\begin{aligned} \sigma_{\text{ppt}} &= 1000 \times \frac{\sigma_{\text{obs}}}{{}^{45}R_{\text{act}}} \\ &= 1000 \times \sqrt{\left(\frac{\sigma_{45}}{A_{45}}\right)^2 + \left(\frac{\sigma_{44}}{A_{44}}\right)^2} \end{aligned} \quad (11)$$

At natural abundance, $A_{45} \sim 0.011A_{44}$. Assuming the feedback resistance is 100× larger for the 45 cup than for the 44 cup, $\Delta_{45} = 0.01\Delta_{44}$. Combining this and Eqs. (5), (8) and (11), we arrive at:

$$\sigma_{\text{ppt}} = \frac{276W\Delta_{44}E}{[{}^{44}\text{CO}_2]N_a e R_\Omega} \quad (12)$$

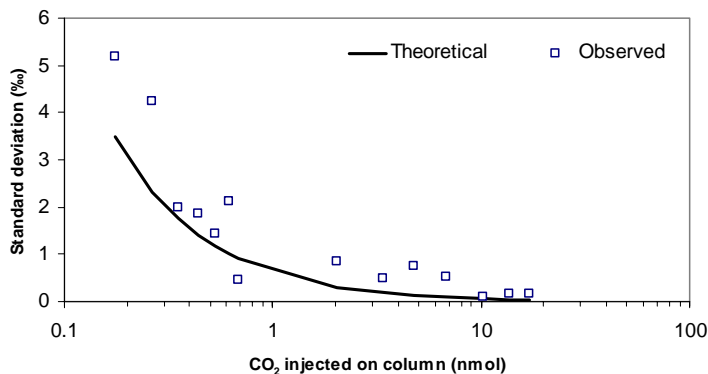


Fig. 6. S.D. ($\delta^{13}\text{C}_{\text{pdb}}$) vs. CO_2 injected on column for simulated 16-bit data. The line indicates the theoretical limit of precision as a function of injection size, as calculated from Eq. (12).

At natural abundance, a standard deviation of $\sigma_{\text{ppt}} = 1.0$ is approximately equivalent to S.D. ($\delta^{13}\text{C}_{\text{pdb}}$) = 1.0‰. We used Eq. (12) to predict the standard deviation as a function of injection size at 16-bit resolution, compensating for an open split ratio of 8.4:1. The integration window, W , was assumed to be constant at 10 s, $E = 5000$, and $R_{\Omega} = 3 \times 10^8 \Omega$. A plot of the calculated limits compared to the observed precision at 16 bits is shown in Fig. 6. There is good agreement between theory and experiment. The calculated precision is within a factor of five of the observed precision for all injection sizes. More striking, the calculated precision is a “lower limit”, as nearly all the measured precisions lie above the theoretical prediction. The biggest discrepancies occur for large injection sizes, where the effect of quantization error is minimized, and other sources of error (e.g. contaminants) may dominate.

Eq. (12) can also be used to demonstrate that quantization error should be negligible for signals acquired with 24-bit digitizers. Eq. (12) predicts that only 0.6 pmol of CO_2 to the IRMS should be necessary to achieve a precision of 0.5‰ if quantization error is the only limiting factor. However, counting statistics dictate that a minimum number of ions must be formed to achieve a specified precision to overcome the shot-noise limit. Merritt and Hayes [11] give this equation as:

$$\sigma_{\delta}^2 = \frac{(2 \times 10^6)(1 + R)^2}{EmN_a R} \quad (13)$$

where σ_{δ} is the shot noise limited standard deviation, R is the natural abundance isotope ratio, E is the ionization efficiency, m is the moles of CO_2 , and N_a is Avogadro’s number. Substituting $E = 5000$ and $R = 0.011$, we find that 6 pmol of analyte is required to achieve S.D. < 0.5‰. Therefore, when high precision 24-bit boards are used, the effect of quantization error is superseded by shot noise.

Our theoretical treatment gives insight into why curve-fitting is less sensitive to quantization error than summation. In the summation methods we have discussed, imprecision in a single data point chosen as the background is multiplied throughout the background correction; for a peak width of N data points, the total quantization error scales as N . In contrast, the algorithms used in curve-fitting minimize the sum of squares between the fit curve and every data point. In curve-fitting, the quantization noise for each individual point is averaged over the entire curve; for N data points, the total quantization error scales as $N^{1/2}$. For a peak width of 10 s and a sampling rate of 10 Hz, this translates into a 10-fold reduction of quantization error.

The theoretical treatment we describe is appropriate for understanding the effects of quantization error on summation integration methods that choose single points on either side of the peak to define a background. It does not examine the limits of other classes of data reduction methods. An obvious improvement to the summation integration method would be to average n points on either side of the peak, which would increase the effective number of bits of

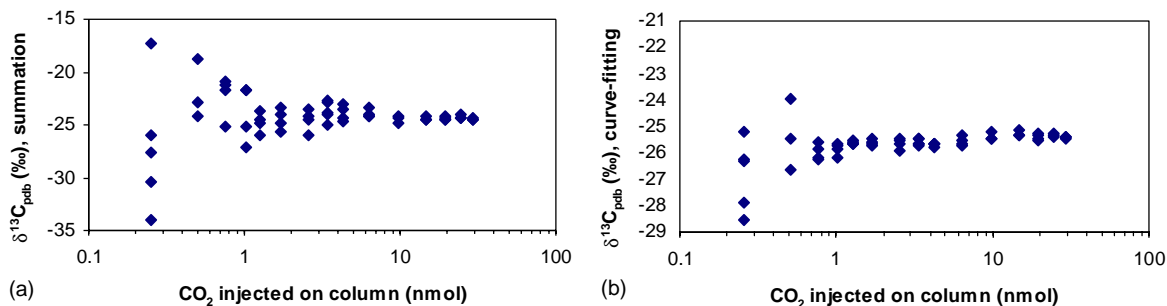


Fig. 7. $\delta^{13}\text{C}_{\text{pdb}}$ vs. CO_2 injected on column for (a) individual summation and (b) curve-fitting algorithms. Data was collected at 16 bits and 10 Hz on the APP2003.

the background measurement by $n^{1/2}$. While this approach could work well for isothermal runs with constant background, it is much less suitable for complex GC–CIRMS chromatograms, where it is not obvious *which* points should be averaged; that is, which points represent pure background and do not contain chemical noise or the tail ends of peaks. Ricci et al., observed that the averaging method gives slightly higher background values than other corrections [3]. They also reported that the dynamic background correction (which uses single points) yielded improved δ -values over the averaging method. Thus, a method may be insensitive to quantization error, but may still give worse results due to other variables.

3.3. Improving precision on a 16-bit IRMS

To test the effectiveness of curve-fitting on GC–CIRMS data acquired by low precision digitiz-

ers, we ran multiple CO_2 injections on an APP2003 using 16-bit digitizers, and otherwise in similar fashion to the work on the FMAT252. A plot of $\delta^{13}\text{C}_{\text{pdb}}$ versus injection size is shown for summation (Fig. 7a) and curve-fitting (Fig. 7b). Fig. 8 shows a plot of S.D. ($\delta^{13}\text{C}_{\text{pdb}}$) as a function of injection size for both integration methods. The theoretical limit on the summation method, calculated from Eq. (12), is shown in the same figure as a dashed line. The observed precision for the summation method agrees well with theoretical predictions; most of the data points lie just above the lower limit curve. Almost 15 nmol of CO_2 on column are necessary to achieve a precision of $<0.3\%$ using the summation method. Using curve-fitting, only 0.76 nmol are necessary to reach that level of precision, a 20-fold improvement. This is greater than the two-fold advantage seen by curve-fitting the 16-bit data from the FMAT 252. One possible explanation is that the APP2003 data is

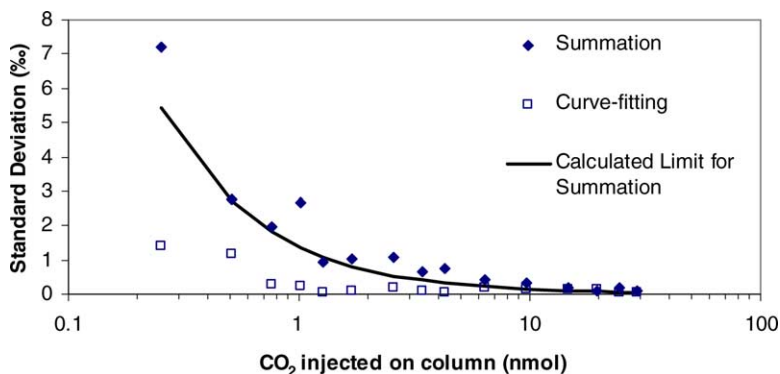


Fig. 8. S.D. ($\delta^{13}\text{C}_{\text{pdb}}$) vs. CO_2 injected on column for runs on APP2003 with 16-bit boards. The dashed line indicates the theoretical limit of quantization error on precision as a function of injection size, as calculated from Eq. (12).

affected primarily by bit noise, while the FMAT252 data has other sources of noise that cannot be eliminated by curve-fitting. The FMAT252 accepts a three-fold higher flow rate than the APP2003, so there is likely more chemical noise in the FMAT252 signal.

The relative immunity to quantization error with curve-fitting permits the IRMS to be run at lower inlet flow rates, which effectively increases quantization noise by decreasing the number of steps between background and peak with relatively little influence on chemical noise. The advantages of lower inlet flow rates are a longer lifetime for the filament, and reduced need for pumps and pumping capacity. These benefits, plus the reduced need for expensive ADC boards, should make high-precision GC–CIRMS more amenable to portable and low-cost applications. In principle, statistical considerations define the lower limits of flow rates. However, counting statistics dictate that S.D. = 0.5‰ requires 6 pmol of CO₂ to the source for a typical continuous flow IRMS ($E = 5000$), and GC–CIRMS applications usually work well above this limit. Thus, modestly lower resolution and inlet flow rates should not significantly affect performance, so long as appropriate integration techniques are used.

4. Conclusions

Data reduction using curve-fitting is more robust than the conventional summation method in the presence of even modest levels of quantization error. Using data obtained on high precision digitizers, the curve-fitting algorithm required several-fold less CO₂ to reach benchmarks of high precision (S.D. = 0.3, 0.6, and 1.0‰) at any of the three simulated board depths (12, 14, or 16 bits). The poor performance of the summation algorithm was particularly noticeable at the 12-bit resolution, where S.D. < 1.0‰ could not be reached even at the maximum injection size allowed by the dynamic range of the Faraday cups. We

have derived an expression that describes the influence of quantization noise on isotope ratios calculated from raw IRMS data, and shown that it accurately predicts the lower limit of precision. Our theoretical treatment assumes that quantization error is uncorrelated between the $m/z = 44$ and 45 signals, and is appropriate for any data reduction algorithm that uses single points on either side of the peak to describe the background.

Curve-fitting substantially improved precision on GC–CIRMS data collected by an instrument with 16-bit digitizers. The summation algorithm required 15 nmol of CO₂ on-column to achieve a precision of S.D. = 0.3‰, while curve-fitting required only 0.76 nmol. Thus, IRMS with 16-bit ADC boards achieved high precision for less than 1 nmol of C on column, a common benchmark for GC–CIRMS applications, despite using 16-bit ADC boards. Lower inlet flow rates, enabling reduced pumping requirements, may be an important advantage in some applications.

References

- [1] W. Meier-Augenstein, *J. Chromatogr. A* 842 (1999) 351.
- [2] J.T. Brenna, T.N. Corso, H.J. Tobias, R.J. Caimi, *Mass Spectrom. Rev.* 16 (1997) 382.
- [3] M.P. Ricci, D.A. Merritt, K.H. Freeman, J.M. Hayes, *Org. Geochem.* 21 (1994) 561.
- [4] K.J. Goodman, J.T. Brenna, *J. Chromatogr. A* 689 (1995) 63.
- [5] K.J. Goodman, J.T. Brenna, *Anal. Chem.* 66 (1994) 1294.
- [6] K.J. Goodman, J.T. Brenna, *Anal. Chem.* 64 (1992) 1088.
- [7] G.L. Sacks, J.T. Brenna, J.T. Sepp, in: *Proceedings of the 49th ASMS Conference on Mass Spectrometry*, Chicago, IL, 2001.
- [8] National Instruments, Austin, TX, 2000.
- [9] N. Dyson, *Chromatographic Integration Methods*, Royal Society of Chemistry, Cambridge, UK, 1990.
- [10] J. Santrock, S.A. Studley, J.M. Hayes, *Anal. Chem.* 57 (1985) 1444.
- [11] D.A. Merritt, J.M. Hayes, *Anal. Chem.* 66 (1994) 2336.
- [12] S. Haykin, *An Introduction to Analog and Digital Communications*, Wiley, New York, 1989.